ACCEPTED FOR PUBLICATION IN APJL
Preprint typeset using LaTeX style emulateapj v. 10/09/06

NON-DETECTION OF GRAVITATIONALLY REDSHIFTED ABSORPTION LINES IN THE X-RAY BURST SPECTRA OF GS 1826–24

ALBERT K. H. KONG[1,2], JON M. MILLER[3], MARIANO MENDEZ[4], JEAN COTTAM[5], WALTER H. G. LEWIN[1], FREDERIK PAERELS[6], ERIK KUULKERS[7], RUDY WIJNANDS[8], AND MICHIEL VAN DER KLIS[8]

Accepted for publication in ApJL

ABSTRACT

During a 200 ks observation with the *XMM-Newton* Reflection Grating Spectrometer, we detected 16 type-I X-ray bursts from GS 1826–24. We combined the burst spectra in an attempt to measure the gravitational redshifts from the surface of the neutron star. We divided the composite GS 1826–24 burst spectrum into three groups based on the blackbody temperature during the bursts. The spectra do not show any obvious discrete absorption lines. We compare our observations with those of EXO 0748–676.

Subject headings: binaries: close—stars: individual (GS 1826–24)—stars: neutron stars—X-rays: binaries—X-rays: bursts

1. INTRODUCTION

The physical properties of neutron stars can be described by an equation of state. For a given equation of state one can obtain a unique relation between mass and radius. Observational constraints on the mass-radius relation of neutron stars can be estimated by a number of methods. One possible way is to measure spectral lines in X-ray burst spectra (Lewin 1993). Absorption features at 4.1 keV (Waki et al. 1984; Nakamura, Inoue, & Tanaka 1988; Maginer et al. 1989) and 5.7 keV (Waki et al. 1984) were reported in X-ray burst spectra with *Tenma* and *EXOSAT*. However, they were never confirmed with more sensitive instruments.

During a 335 ks observation made in the calibration phase of *XMM-Newton*, 28 type-I X-ray bursts were detected from EXO 0748–676. Cottam, Paerels & Mendez (2002) reported features in the bursts spectra of this source which they interpreted as gravitationally redshifted absorption lines of Fe XXVI during the early phase of the bursts, and Fe XXV and perhaps O VIII during the late phase. The lines would then have all a gravitational redshift of $z = 0.35$, which would correspond to a neutron star in the mass range of 1.4–1.8 $M_{\odot}$ and in the radius range of 9–12 km (see also van Paradijs & Lewin 1987; Özel 2006). If confirmed, these detections might rule out soft equations of state for neutron star matter (Özel 2006). This is potentially very exciting, however, it still needs to be confirmed that these features in EXO 0748–676 are gravitational redshifted absorption lines, either by observing it in an independent data set of the same source or observing similar features in the burst spectra of other systems. Before the above results from EXO 0748–676 were known, *XMM-Newton* observations of the X-ray burster GS 1826–24 were requested in October 2001 (PI: Lewin) to search for gravitationally redshifted lines in X-ray burst spectra.

GS 1826–24 is an ideal source for studying thermonuclear X-ray bursts because of its bright, long, and regular bursts (Galloway et al. 2004; Kong et al. 2000). The bursts have recurrence times between ~ 3.5 hr and ~ 5.7 hr (Cornelisse et al. 2003; Galloway et al. 2004). We report here on the results of our 200 ks *XMM-Newton* observations.

2. OBSERVATIONS AND DATA REDUCTION

GS 1826–24 was observed with *XMM-Newton* two times on 2003 April 6–8 (108 ks) and April 8–9 (92 ks) during which a total of 16 type-I X-ray bursts were observed with a recurrence time of ~ 3.1 hr. Both the European Photon Imaging Camera (EPIC) and the Reflection Grating Spectrometer (RGS) were turned on; the Optical Monitor was turned off during the observations. In this paper, we present the high resolution X-ray spectra from the RGS. We used the EPIC data only for identifying bursts and examining the burst profiles. The RGS covers the energy range from 5 to 35 Å (0.35–2.5 keV) with a resolving power of ~ 400 at 15 Å. The EPIC consists of three detectors (one pn camera and two MOS cameras) sensitive between 0.2 and 15 keV. In this analysis, we only used data from the pn detector (with the thin filter and in timing mode). The data were processed with the *XMM-Newton* Science Analysis System (SAS) version 7.0. We performed spectral analysis by using XSPEC v11.

3. RESULTS

3.1. *Burst Profiles and Broadband Spectra*

We plot the burst profiles of the 16 bursts in Figure 1; they are very similar for all bursts. As during all previous observations with other instruments (Kong et al. 2000; Galloway et al. 2004), the bursts show a fast rise, followed by an exponential decay; typical burst durations were ~ 200 s. Using the EPIC-pn data, we extracted the time-resolved 0.3–10 keV spectra with 5-s time resolution in the rising phase and 10-s resolution during decay. We chose a 2000-s section of data prior to the bursts which we used as our "background" for spectral fits to the individual spectra of the bursts. The response matrices were created with SAS together with the latest calibration products. The net burst–background emission was well fitted

[1] Kavli Institute for Astrophysics and Space Research, Massachusetts Institute of Technology, 77 Massachusetts Avenue, Cambridge, MA 02139
[2] Department of Physics and Institute of Astronomy, National Tsing Hua University, Hsinchu, Taiwan; akong@phys.nthu.edu.tw
[3] Department of Astronomy, University of Michigan, Ann Arbor, MI 48109
[4] SRON, Netherlands Institute for Space Research, Sorbonnelaan 2, 3584 CA Utrecht, Netherlands
[5] Exploration of the Universe Division, NASA Goddard Space Flight Center, Greenbelt, MD 20771
[6] Columbia Astrophysics Laboratory, Columbia University, 550 West 120th Street, New York, NY 10027
[7] ISOC, ESA/ESAC, Urb. Villafranca del Castillo, PO Box 50727, 28080 Madrid, Spain
[8] Astronomical Institute "Anton Pannekoek," University of Amsterdam, Kruislaan, Amsterdam, Netherlands

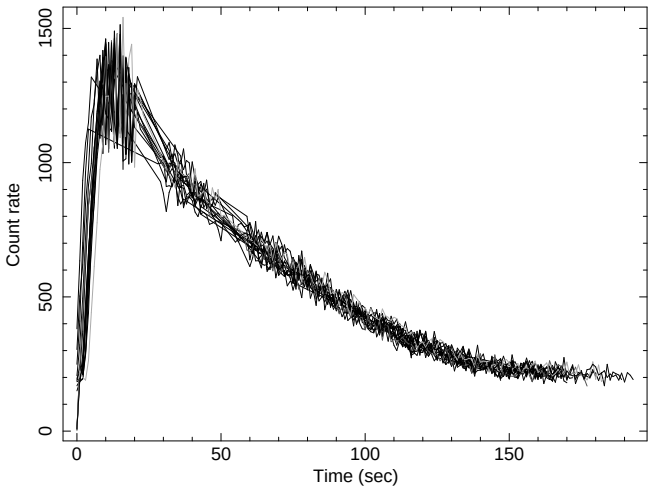

FIG. 1.— Lightcurves of all X-ray bursts detected with the *XMM-Newton* pn detector. The missig data during decay are due to telemetry deadtime. All bursts have a similar fast rise followed by an exponential decay; burst durations were ~ 200 s.

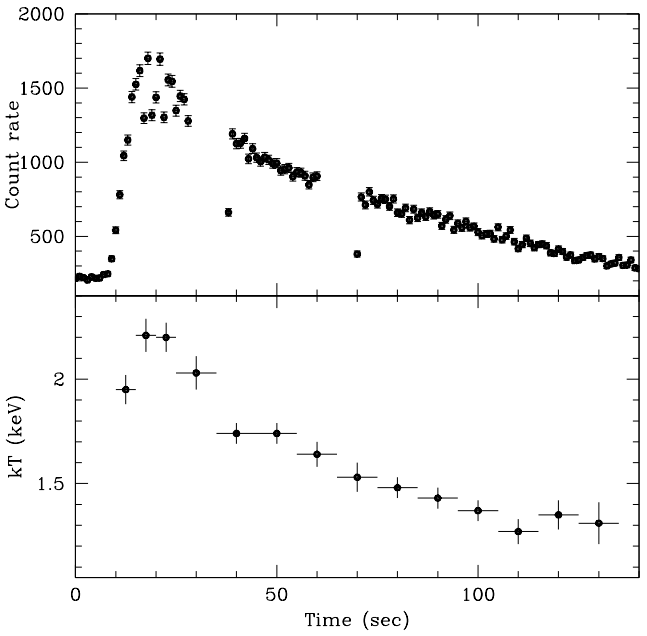

FIG. 2.— A representative burst profile (Upper panel) and temperature profile (Lower panel) from GS 1826–24 as observed with the EPIC-pn. The time resolution for the lightcurve is 1 s. Drops in count rate are due to telemetry deadtime. The rising and decay phase of the temperature profile has a time resolution of 5 s and 10 s, respectively. The missing data do not show in the temperature profile because the time resolution of the two plots is different.

with a simple blackbody model. The burst and temperature profiles are plotted in Figure 2.

3.2. *RGS Burst Spectra*

We used the EPIC-pn light curve as a guide to extract the first-order RGS spectra for each burst. Since the spectral properties are changing during the bursts (see Fig. 2), we studied the RGS spectra separately according to the blackbody temperatures as derived from the EPIC-pn data. In Figure 3, we show the correlation between the blackbody temperatures and count rates of all bursts. A strong positive correlation is found between the two quantities indicating that the properties are very similar for all bursts. Using this correlation as a reference, we divided the bursts into three phases: $kT < 1.5$ keV, 1.5 keV $< kT < 2$ keV, and $kT > 2$ keV. We note that the division we used here is different from that in the study of EXO 0748–676 (Cottam et al. 2002) in which the bursts were divided into "early" and "late" phases.

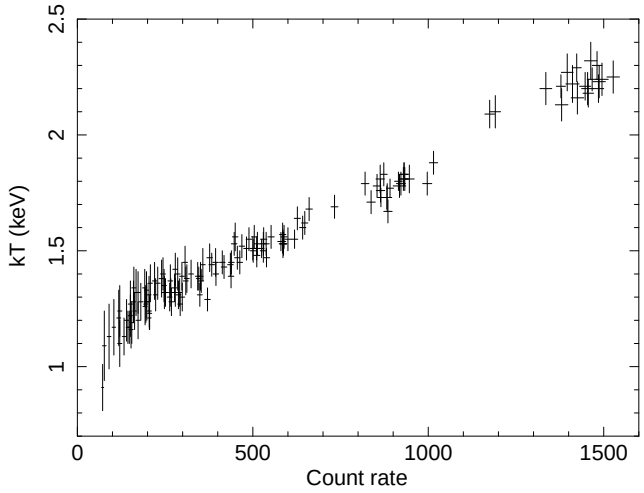

FIG. 3.— Correlation between the blackbody temperatures and count rates of all bursts detected with EPIC-pn.

For each observation, and for each RGS camera, we extracted three separate first-order spectra of the bursts according to their blackbody temperature as determined by the EPIC-pn count rate (Fig. 3). For each RGS camera we used the same response matrix for each observation. Finally, we created background spectra using spatially offset regions. We then used the task *rgscombine* in the SAS software to combine the three RGS spectra of the two observations separately for each RGS camera. We ended up with 6 spectra in total, one for each interval of the blackbody temperature of the bursts in each of the two RGS cameras. Since all bursts are statistically indistinguishable, for each temperature interval we combined the spectra of both RGS cameras using the SAS command *rgsfluxer*. In Figure 4 we plot the background-subtracted spectra for the three phases of the average burst. Above 27 Å the flux drops significantly due to the effect of the interstellar absorption.

We rebinned the spectra with at least 20 counts per spectral bin, and used χ^2 statistics to find the best-fitting parameters. All three spectra can be adequately fitted with an absorbed blackbody model with a reduced χ^2 of ~ 1. There is no evidence for absorption edges apart from those due to the ISM (oxygen and neon are the most prominent). Any real absorption line must be seen in both RGS spectra where there is simultaneous wavelength coverage. The only possible line significant at the 3σ level of confidence or higher is Ne X Ly-α (theoretical wavelength: 12.1339Å), though it falls in a range covered by only one RGS spectrum. Fits with a Gaussian measure a wavelength of $12.16^{+0.02}_{-0.06}$Å and an equivalent width of 80^{+30}_{-20} mÅ (1σ errors). The FWHM is consistent with zero, indicating the line is not resolved. Via an F test, the line is significant at the 3.4σ level of confidence. The line cannot be tied to the stellar surface or even clearly tied to a wind as its observed wavelength is consistent with zero shift, though Ne X is seen in some disk winds (Miller et al. 2006).

To compare our analysis with EXO 0748–676, we also fitted the three burst spectra with a circumstellar model similar to that used by Cottam et al (2002). We used a continuum model consisting of power-law emission with neutral inter-

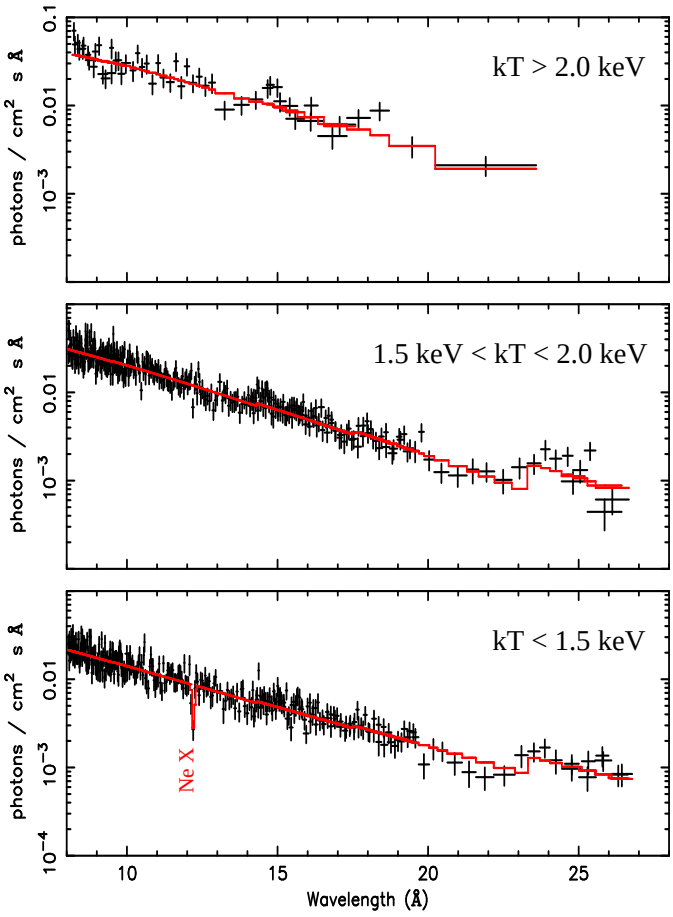

FIG. 4.— *XMM-Newton* RGS average background subtracted spectra for 16 X-ray bursts from GS 1826–24. The three temperature phases are defined according to the spectral fits with the EPIC-pn data. An absorbed blackbody model is superimposed in red. The Ne X line at 12.1 Å (with 3.4σ confidence) is included in the low-temperature spectrum.

stellar absorption and then added in absorption models for each of the following ions: N VI, N VII, O VII, O VIII, Ne IX, and Ne X. We do not intend to establish a definitive spectral fit, but rather to determine which features might be circumstellar in origin. We therefore required that all ions be generated at the same plasma temperature and redshift, but we allowed the ion abundances to float. This provided an estimate of the circumstellar contributions to the spectra, but it does not necessarily provide a physically realistic circumstellar model for the source. This fitting process provides a reasonable estimate for the lower and medium-temperature spectra; the high-temperature spectrum has a low signal-to-noise ratio and is difficult to reproduce with the Cottam et al. (2002) model. After fitting the circumstellar contributions to the observed burst spectra, we searched for residual spectral features that might be generated in the neutron star photosphere. We do not find any obvious neutron star photospheric absorption features in these spectra, consistent with the simple absorbed blackbody model.

In order to obtain upper limits in the equivalent widths of our data in the lines reported in Cottam et al. (2002), we assume a Gaussian function centered at between 10–14 Å with a width of 0.1 – 0.3 Å. We note that the width of the lines reported in EXO 0748–676 is about 0.11 Å (from unpublished results in Cottam et al. 2002). Using these assumptions as well as the low-temperature spectrum, we can set a 90% confidence limit to the equivalent width of 0.24 Å for any absorption line between 10 and 14 Å.

4. DISCUSSION

We observed GS 1826–24 with the *XMM-Newton* RGS and detected 16 type-I X-ray bursts. We note that we are not less sensitive than the results by Cottam et al. (2002). The reported features from EXO 0748–676 are from composite spectra of 28 bursts while we only detected 16 bursts. However, the total number of counts in the spectra is comparable because of the longer burst durations in GS 1826-24; the burst peak intensities were similar. By adding all the burst spectra, the high resolution *XMM-Newton* RGS spectra can be fitted with a simple absorbed blackbody model and show no obvious absorption features (see Figure 4). We do not see in GS 1826–24 features similar to the ones seen by Cottam et al. (2002) in EXO 0748–676 which they interpreted as the Fe XXVI and XXV n=2-3 transitions with a redshift of $z = 0.35$. For comparison, the equivalent widths of Fe XXV and Fe XXVI lines reported in Cottam et al. (2002) are 0.18 Å and 0.13 Å, respectively while we obtained a 90% upper limit of 0.24 Å for any absorption line between 10–14 Å with a width of 0.1–0.3 Å. However, if the line width is similar to EXO 0748–676 at 0.11 Å, the 90% upper limit of the equivalent width becomes 0.13 Å. We note that follow-up observations of EXO 0748–676 have failed to again reveal absorption lines from the stellar surface (Cottam et al. 2007).

If the features initially seen in EXO 0748–676 are real and are due to absorption lines redshifted by the gravity of the neutron star, then it is important to determine why we do not see similar phenomena in our burst spectra from GS 1826–24. Absorption features in burst spectra are very sensitive to the accretion rate, temperatures, density, and the rotation frequency of the neutron star (Bildsten, Chang & Paerels 2003; Chang, Bildsten & Wasserman 2005; Chang et al. 2006). For instance, the different absorption features during the early phase and late phase of the burst spectra seen from EXO 0748–676 may be due to a change in ionization balance of iron in the photosphere. In the case of EXO 0748–676, the EPIC-pn burst spectra show a peak temperature of about 1.8 keV and the temperature drops to 1.5 keV during burst decay. For GS 1826–24 the peak temperature of the bursts is about 2.3 keV (see Figure 2). During decay, the temperature drops to about 1.3 keV. The peak temperature of bursts from GS 1826–24 is higher than that from EXO 0748–676. This may explain why we do not see any absorption features in the spectrum of burst data in excess of 2 keV. However, the burst temperatures during our low- and medium-temperature spectra are similar to those observed during the decay and peak of the bursts from EXO 0748–676. We might therefore expect to see absorption features in our spectra.

Rotational broadening may explain the absence of absorption features in GS 1826–24 burst spectra as it will modify the line profile (Özel & Psaltis 2003). Chang et al. (2005) calculated that for an edge-on neutron star with a rotation rate > 200 Hz, the absorption features would become undetectable. Thompson et al. (2005) reported a possible burst oscillation in GS 1826–24 at ~ 611 Hz, which, if proven to be true, would make the absorption lines less likely to be detected. EXO 0748–676, however, is a very slow rotator with a rotation rate of 44.7 Hz (Villarreal & Strohmayer 2004). More recently, Chang et al. (2006) fitted the line profiles of EXO 0748–676 with a theoretical model including the effect

of rotational broadening; they reported a gravitational redshift of $z = 0.345^{+0.005}_{-0.008}$ (95% confidence). However, they showed that rapid rotation does not necessarily make spectral lines undetectable. If a rapidly rotating neutron star is seen face-on, the spectral lines will be narrower. EXO 0748–676 is an edge-on source while GS 1826–24 has an inclination angle $< 70^\circ$ (Homer, Charles, & O'Donoghue 1998). A theoretical study shows that narrow lines can be detected even at spin frequencies as high as 600 Hz for emission near the rotation axis (Bhattacharyya et al. 2006). It is therefore uncertain whether a possible high spin frequency of the neutron star could be the cause of the non-detection of spectral lines in GS 1826–24 since most accreting neutron stars for which the spin has been determined have a spin frequency < 600 Hz (e.g., van der Klis 2006).

The chemical composition of the atmosphere of the neutron star is another factor that can influence the line profiles (Chang et al. 2005). A more detailed theoretical study of line profiles in a mixed Hydrogen/Helium environment is required to examine the effect on the ionization balance (see Bildsten 2000).

We also have to consider the possibility that the lines seen in EXO 0748-676 are not gravitational redshifted iron lines from the surface. EXO 0748–676 is a high inclination system and shows large dips in the X-ray light curve due to an absorbing medium in the outer accretion disk, far from the inner part of the system. Homan, Wijnands, & van den Berg (2003) proposed that a large fraction of the bursts used by Cottam et al. (2002) occurred during times of significant absorption at low energies (< 2 keV) due to obscuring medium in the outer disk. This might have introduced absorption features in the burst spectra which could be due to the material inside the obscuring matter and not due to material on the surface of the neutron star. However, it is difficult to associate the lines seen in the burst spectra of EXO 0748–676 with He-like or H-like lines from abundant elements unless large velocity shifts are invoked. In contrast, if obscuration in the outer disk drives dipping behavior, small velocity shifts would be expected. On balance, it is not clear that obscuration in the outer disk could produce the absorption lines observed.

Additional observations of burst sources with *XMM-Newton* can help to better understand the conditions in which lines in X-ray bursts are strongest. Future X-ray missions with high collecting area and high spectral resolution such as *Constellation-X* and *XEUS* are ideally suited to detecting absorption lines from the surface of neutron stars. We ultimately look forward to definitive observations with these missions.

This work is based on observations obtained with *XMM-Newton*, an ESA mission with instruments and contributions directly funded by ESA member states and the US (NASA). W.H.G.L. gratefully acknowledges support from the NASA.

Facilities: XMM (EPIC, RGS)

REFERENCES

Bhattacharyya, S., Miller, M. C., & Lamb, F. K. 2006, ApJ, 644, 1085
Bildsten, L. 2000, American Institute of Physics Conference Series, 522, 359
Bildsten, L., Chang, P., & Paerels, F. 2003, ApJ, 591, L29
Chang, P., Morsink, S., Bildsten, L., & Wasserman, I. 2006, ApJ, 636, L117
Chang, P., Bildsten, L., & Wasserman, I. 2005, ApJ, 629, 998
Cornelisse, R., et al. 2003, A&A, 405, 1033
Cottam, J., Paerels, F., & Mendez, M. 2002, Nature, 420, 51
Cottam, J., Paerels, F., Mendez, M, Boirin, L., Lewin, W. H. G., Kuulkers, E., Miller, J. M. 2007, ApJ, in press, arXiv:0709.4062
Galloway, D. K., Cumming, A., Kuulkers, E., Bildsten, L., Chakrabarty, D., & Rothschild, R. E. 2004, ApJ, 601, 466
Homer, L., Charles, P. A., & O'Donoghue, D. 1998, MNRAS, 298, 497
Homan, J., Wijnands, R., & van den Berg, M. 2003, A&A, 412, 799
Kong, A. K. H., Homer, L., Kuulkers, E., Charles, P. A., & Smale, A. P. 2000, MNRAS, 311, 405
Lewin, W. H. G. 1993, AIP Conference Proceedings, 308, The Evolution of X-ray Binaries, eds. S. Holt & C. Day, page 3–17
Magnier, E., Lewin, W. H. G., van Paradijs, J., Tan, J., Penninx, W., & Damen, E. 1989, MNRAS, 237, 729
Miller, J. M., Raymond, J., Fabian, A., Steeghs, D., Homan, J., Reynolds, C., van der Klis, M., & Wijnands, R. 2006, Nature, 441, 953
Nakamura, N., Inoue, H., & Tanaka, Y. 1988, PASJ, 40, 209
Özel, F., & Psaltis, D. 2003, ApJ, 582, L31
Özel, F. 2006, Nature, 441, 1115
Thompson, T. W. J., Rothschild, R. E., Tomsick, J. A., & Marshall, H. L. 2005, ApJ, 634, 1261
van der Klis, M. 2006, Compact stellar X-ray sources, 39
van Paradijs, J., & Lewin, W. H. G. 1987, A&A, 172, L20
Villarreal, A. R., & Strohmayer, T. E. 2004, ApJ, 614, L121
Waki, I., et al. 1984, PASJ, 36, 819